

KATIRA ET AL

**ADVERSE HEART-LUNG INTERACTIONS IN VENTILATOR-INDUCED LUNG INJURY**

Bhushan H Katira<sup>1,2,3</sup>, Regan E Giesinger<sup>4</sup>, Doreen Engelberts<sup>1</sup>, Diana Zabini<sup>5</sup>, Alik Kornecki<sup>1</sup>, Gail Otulakowski<sup>1</sup>, Takeshi Yoshida<sup>1,2,3</sup>, Wolfgang M Kuebler<sup>5,6</sup>, Patrick J McNamara<sup>4</sup>, Kim A Connelly<sup>5</sup>, Brian P Kavanagh<sup>1,2,3</sup>

**Affiliations:** Translational Medicine, The Research Institute, Hospital for Sick Children, Toronto, Canada; <sup>2</sup>Departments of Critical Care Medicine and Anesthesiology, Hospital for Sick Children, University of Toronto, Toronto, Canada; <sup>3</sup>Interdepartmental Division of Critical Care Medicine, University of Toronto, Toronto, Canada; <sup>4</sup>Division of Neonatology, Department of Pediatrics, Hospital for Sick Children, University of Toronto, Toronto, Canada; <sup>5</sup>Keenan Research Centre for Biomedical Sciences, St. Michael's Hospital, Toronto, Canada; <sup>6</sup>Departments of Surgery and Physiology, University of Toronto, Toronto, Canada.

**Correspondence:** Dr. Kavanagh (brian.kavanagh@utoronto.ca)

**Support:** Supported by research funds (BPK) from the Canadian Institutes of Health Research. BPK holds the Dr Geoffrey Barker Chair in Critical Care Research. KAC holds a New Investigator reward from the Canadian Institutes of Health Research and an Early Researcher Award from the Ministry of Research and Innovation and Science, Ontario.

**Author Contributions:** *Conception and design:* BHK, REG, DE, DZ, AK, GO, TY, WMK, PJM, KAC, BPK; *Analysis and interpretation:* BHK, REG, DE, DZ, AK, GO, TY, WMK, PJM, KAC, BPK; *Drafting the manuscript for important intellectual content:* BHK, REG, DE, DZ, AK, GO, TY, WMK, PJM, KAC, BPK

**Manuscript** 3,863 words

**Abstract** 254 words

**Tables** 2

**Figures** 5

**References** 51

**On-Line Supplement:** Tables 5; Figures 5

KATIRA ET AL

**What is known about this Topic:** A classic study (Webb & Tierney 1974) of ventilation with high tidal volume and zero PEEP concluded that the resulting severe lung injury was due to vascular interdependence and surfactant depletion. Later studies confirmed these findings and reported major permeability alterations and severe ultrastructural damage likely due to shear stress. These experimental and highly cited works on ventilation-induced lung injury prompted key clinical studies that have changed practice in ARDS.

**What this Study adds:** We reproduced the key findings of a classic model of VILI with high peak pressure and zero PEEP, and show respiratory swings in RV filling and pulmonary perfusion, with both obliterated during peak inspiration. RV systolic pressure, initially maintained, progressively decreases and is ultimately associated with marked RV dilation; and, a modest (approximately 40%) increase in transmural LVEDP. All of these effects were prevented by addition of PEEP. The mechanism of the acute *cor pulmonale* is uncertain but might be due to pulmonary microvascular injury from cyclic interruption/exaggeration of flow.

**ABSTRACT (254 words)**

**RATIONALE:** The original *in vivo* study of ventilator-induced lung injury by Webb and Tierney (1974) reported that high  $V_T$  with zero PEEP caused overwhelming lung injury, subsequently shown by others to be due to lung shear stress.

**OBJECTIVE:** To reproduce the lung injury and edema in the ‘Webb and Tierney’ study and investigate the mechanism.

**METHODS:** Sprague-Dawley rats ( $\approx 400$  g) received mechanical ventilation for 60 min according to the protocol of Webb and Tierney (14/0, 30/0, 45/10, 45/0 cmH<sub>2</sub>O). Additional series of experiments (20 min duration, to ensure all animals survived) were studied to assess permeability (4/group), echocardiography (4/group), and right and left ventricular pressure (5 and 4/group, respectively).

**MEASUREMENTS AND MAIN RESULTS:** The original Webb & Tierney results were replicated in terms of lung/body weight ratio (45/0 > 45/10  $\approx$  30/0  $\approx$  14/0;  $P < 0.05$ ), and histology. In 45/0, pulmonary edema was overt and rapid, with survival less than 30 min. In 45/0 (but not 45/10), there was an increase in microvascular permeability, cyclical abolition of preload, and progressive dilation of the right ventricle. While left ventricular end-diastolic pressure decreased in 45/10, it increased in 45/0.

**CONCLUSIONS:** In a classic model of VILI high peak pressure (and zero PEEP) causes respiratory swings (obliteration during inspiration) in RV filling and pulmonary perfusion, and ultimate RV failure and dilation. Pulmonary edema was due to increased permeability, augmented by a modest (approximately 40%) increase in hydrostatic pressure. The mechanism of *cor pulmonale*

*KATIRA ET AL*

is uncertain but might be due to pulmonary microvascular injury from cyclic interruption/exaggeration of flow.

## INTRODUCTION

There is overwhelming evidence from randomized trials that mechanical ventilation contributes to mortality in patients with ARDS (1, 2). These trials were based on earlier clinical studies (3, 4) that in turn were based on laboratory data from the 1960s to 1980s, indicating that MV could directly injure lungs (5-9).

Mechanical ventilation was first reported to cause surfactant depletion and atelectasis by Greenfield *et al* in 1964 (10) and Faridy *et al* (11). Webb and Tierney, in their highly cited 'classic' paper published in 1974, used the *in vivo* rat to demonstrate fulminant pulmonary edema following high tidal volume (and protection by PEEP) (12). Subsequently Egan *et al* and Parker *et al* reported increased permeability (7, 13-15). Dreyfuss *et al* reported increased microvascular permeability and endothelial lesions (8), and later they (16) and Hernandez *et al* (17) prevented injury by restricting chest wall expansion. VILI was associated with edema due to elevated capillary hydrostatic pressure ( $P_{mv}$ ), a phenomenon attributed to unrestricted RV filling in the open chest model (18); however, PEEP prevented edema formation in the setting of high peak airway pressure, and because dopamine administration increased edema, this suggested a role for pulmonary microvascular pressure ( $P_{mv}$ )(19)

In pilot experiments, we reproduced the classic study of Webb and Tierney (12) and confirmed the previously reported precipitous pulmonary edema (in 45/0). This prompted us to wonder about a cardiac contribution. We therefore reproduced the experiments and determined the effect and contribution of right ventricular function in this model of VILI.

## METHODS

Healthy adult male Sprague-Dawley Rats (Charles River Montreal, QC, Canada; 350-500 gm) were used in all experiments. Institutional Ethics approval (conforming to the guidelines of the Canadian Council on Animal Care) was obtained. After inducing anesthesia, venous access, tracheostomy and carotid artery cannulation were performed. Airway and arterial pressure were continuously monitored and anesthesia maintained with continuous infusion of Ketamine and Xylazine as previously described (20).

**Experimental Series 1 - Replication of original Study by Webb and Tierney:** Animals were ventilated with baseline settings (tidal volume,  $V_T$  6 mL·kg<sup>-1</sup>; 60 min<sup>-1</sup>; FiO<sub>2</sub> 0.21; PEEP 3 cmH<sub>2</sub>O) and baseline parameters recorded. After stabilization, animals (5 per group) were randomized to one of the following groups, defined by airway pressure ( $P_{aw}$ ) as: 14/0, 30/0, 45/0 or 45/10 cmH<sub>2</sub>O. The peak inspiratory/end-expiratory pressures (and corresponding 'delta' pressures) were: 14/0 (14), 30/0 (30), 45/0 (45), and 45/10 (35) cmH<sub>2</sub>O. While the original study (12) randomized to 6 groups (Control, 14/0, 30/0, 30/10, 45/0 or 45/10 cmH<sub>2</sub>O), the current study omitted 'control' (*i.e.* non-ventilated) and 30/10 groups, as they were not a focus. Ventilation was for 1 hour (or until death, whichever occurred earlier).  $V_T$  was adjusted to maintain assigned  $P_{aw}$ , as in the original study (12), and respiratory rate adjusted to maintain normal PaCO<sub>2</sub>. Dead-space (3 mL) was added in 45/0 and 30/0. Arterial blood gases (ABG) were measured at baseline (before randomization), and (with dynamic compliance,  $C_{Dyn}$ ) at the start and end of the experiment. The duration of the experiments 1 hour for groups 14/0, 30/0 and 45/10; for 45/0, the experiment was terminated when the mean arterial pressure was 20 mmHg. After the experiment was complete, lungs were removed and weighed, and the lung to

body weight ratio (LBW) determined. In selected animals (2/group) the right lung was pressure-fixed (formalin, 25 cmH<sub>2</sub>O) and stained with Haematoxylin-Eosin for blinded histologic scoring (20).

**Experimental Series 2 – Determination of Microvascular Permeability:** Animals were randomized to: 45/0 (n=4), 45/10 (n=4) to assess microvascular permeability to protein, and an additional comparison group (10/3, n=2; control) was included. As in Series 1, the animals were ventilated at baseline settings before randomization (tidal volume, V<sub>T</sub> 6 mL·kg<sup>-1</sup>; 60 min<sup>-1</sup>; FiO<sub>2</sub> 0.21; PEEP 3 cmH<sub>2</sub>O). Evans Blue dye was given intravenously (30 mg·kg<sup>-1</sup>). After randomization, animals were ventilated (FiO<sub>2</sub> 0.21) for 20 mins (to ensure survival in the 45/0 group). Ventilation management, and ABG (and C<sub>Dyn</sub>) measurement was as in Series 1. At the end of the experiment the left lung was removed and the ratio of wet-to-dry weight calculated (W/D ratio). Right lung lavage was performed with saline (5 mL, repeated x3) and the bronchoalveolar lavage (BAL) collected was analysed for Evans Blue dye absorbance using photo-spectrometry (21).

**Experimental Series 3 – Echocardiographic Studies:** Animals were randomized to: 45/0 (n=4), 45/10 (n=4) to assess echocardiography (GE Vivid 7, 10 MHz probe). Echocardiography was performed at baseline, start and 20 minutes. Ventilation management and measurement was as in Series 2. The image acquisition plane was standardized (22) and image landmarks remained stable to ensure that a consistent view remained in focus. Inclusion was limited to images where the field of view and Doppler planes were within the standard range. Right ventricular output was calculated using the formula:  $CO = ([3.14 \times VTI \times HR \times \pi R^2]/W)$ , where: VTI velocity time integral; HR heart rate; R radius of pulmonary artery; and, W animal weight.

VTI was measured using pulsed wave Doppler at the level of the hinge points of the pulmonary artery annulus in a parasternal short axis plane, at an angle of insonation <10 degrees (23). The ratio of right ventricular area to left ventricular area was measured at mid-cavity during peak diastole in a parasternal short axis plane at the level of the tips of the mitral valve leaflets. Right ventricular ejection time (RVET) and pulmonary artery acceleration time (PAAT) were measured using pulsed wave Doppler and their ratio determined (a surrogate of pulmonary vascular resistance). The eccentricity index of the left ventricle was calculated in systole and diastole and fractional shortening determined by m-mode in a parasternal short axis plane (24). Tricuspid annular plane systolic excursion (TAPSE, a parameter of global RV function) was determined using m-mode in the four chamber view (25).

**Experimental Series 4 – Right Ventricular Pressure Studies:** Animals were randomized to: 45/0 (n=4), 45/10 (n=4) to assess right ventricular (RV) pressures, and an additional comparison group (10/3, n=2; control) was included. Ventilation management and measurement was as in Series 2. A Millar catheter (SPR-407/AD Instruments, CO, USA) was inserted *via* the internal jugular vein into the right ventricle to measure right ventricular pressure (RVP). Esophageal manometry ( $P_{ES}$ ) was performed using a water filled catheter placed in the lower esophagus as previously described (26). Right ventricular systolic pressure (RVSP) and right ventricular end-diastolic pressure (RVEDP) were noted in inspiration and in expiration.

Transmural (TM) RV pressure was calculated in systole as:  $RVSP-TM = [RVSP - P_{ES}]$ ; and, and at end-diastole as:  $RVEDP-TM = [RVEDP - P_{ES}]$ , during inspiration and during expiration. Right coronary perfusion pressure (RCPP) was calculated as:  $RCPP = [MAP - \text{mean RVP}]$ , where MAP is mean arterial pressure, and RVP is right ventricular pressure (27).

Transpulmonary pressure ( $P_L$ ) was calculated as:  $P_L = [P_{aw} - P_{es}]$ , in inspiration and in expiration;  $\Delta P_L$  was calculated as:  $\Delta P_L = [\text{Inspiratory } P_L - \text{expiratory } P_L]$ .

**Experimental Series 5 – Left Ventricular Pressure (LVP) Studies:** Animals were randomized to: 45/0 (n=4), 45/10 (n=4) to assess left ventricular (LV) pressures, and an additional comparison group (10/3, n=2; control) was included. Ventilation management and measurement was as in Series 2. A Millar catheter was placed in the left ventricle *via* a retrograde right carotid artery approach;  $P_{ES}$  was measured as in Series 4. Left ventricular pressure was measured as an average of 10 beats over a respiratory cycle.

For each beat, transmural (TM) left ventricular pressure was calculated in systole (LVSP) as:  $LVSP-TM = [LVSP - P_{ES}]$ ; and, at end-diastole (LVEDP) as:  $LVEDP-TM = [LVEDP - P_{ES}]$ . Left coronary perfusion pressure (LCPP) was calculated as:  $LCPP = [\text{Diastolic SAP} - LVEDP]$ , where SAP is systemic arterial pressure (27).

**Analysis:** Data were recorded in real time (POWERLAB software, Labchart AD Instruments Denver, CO), were expressed as mean  $\pm$  SD and were compared using 1-way or 2-way ANOVA with statistical significance set at  $P < 0.05$ .

## RESULTS

5 series of experiments were completed.

**SERIES #1:** Four groups were randomized to airway pressures ( $P_{aw}$ ) of: 14/0, 30/0, 45/10 or 45/0 cmH<sub>2</sub>O, in order to reproduce the original experiments of Webb and Tierney (12). 20 animals (5 per group) were studied. Baseline characteristics (e.g. arterial blood gases,  $P_{aw}$ ) were within normal range in all groups (**Table 1-Supplement**).

The target  $P_{aw}$  was reached in each group. The  $V_T$  was highest in 45/0 and in this group,  $C_{Dyn}$  fell between baseline (0 min) and death (**Table 1-Supplement**). By the end of the experiment,  $PaCO_2$  was comparable in all groups, and the rank order of  $PaO_2$  was 14/0  $\approx$  30/0  $\approx$  45/10 > 45/0 (**Table 1-Supplement**). Survival was 100% in all groups except 45/0, in which duration of survival was 15–30 min (mean survival time in 45/0 was 26 $\pm$ 6 min;  $P$ <0.001 vs. other groups).

Pulmonary edema, expressed as the ratio of wet lung weight/body weight (12), was ranked as: 14/0  $\approx$  30/0  $\approx$  45/10 < 45/0, similar to the original study by Webb and Tierney (**Figure 1**). Histology revealed greater alveolar damage, edema and hemorrhage in 45/0 as compared to other groups (**Figure 1-Supplement**; **Table 2-Supplement**).

**SERIES #2:** Animals were randomized to ventilation with 45/0 or 45/10, and ventilation continued for 20 min. A small non-randomized group of 10/3 was included for illustration but excluded from statistical comparisons. Permeability (leak of Evans Blue dye into the BAL fluid) (**Figure 2-A**) and lung W/D ratio (**Figure 2-B**) were significantly higher in 45/0. As in Series 1,  $V_T$  in 45/0 was higher, as was the reduction in  $C_{Dyn}$  between 0 and 20 min. Arterial pH and  $PaO_2$  were significantly lower in 45/0 (**Table 3-Supplement**). In this series, 2 animals in 45/0 survived for 20 min, whereas two experiments were terminated early (at 15 and 18 min).

**SERIES #3:** Animals were assigned to ventilation groups as in Series #2 above. In 45/0, echocardiography at time = 0 min revealed that the RV was markedly under-filled during inspiration, but not during expiration (**Figure 3; Video-supplement**). In contrast, in 45/10 RV filling was constant through inspiration and expiration. The cyclic inspiratory non-filling of the RV in 45/0 was accompanied by cyclic abolition of right ventricular stroke volume (**Table 1**) and pulmonary artery flow. While the pulmonary artery flow was also reduced in 45/10 during inspiration, the magnitude of this effect was less than in 45/0. Right and left ventricular area (surrogate for volume) was less during inspiration vs. expiration in 45/0, but was constant throughout the respiratory cycle in 45/10 (**Table 1**). Over the course of the experiment, the RV became progressively dilated in 45/0, increasing the RV/LV ratio; this did not occur in 45/10 (**Figure 4-A, Table 1**). The ratio of RVET:PAAT was high in 45/0 at 0 min during expiration (**Table 1**). Left ventricular eccentricity index progressively increased in 45/0, especially during systole (**Table 1**). TAPSE declined to a greater extent in 45/0 vs. 45/10 (**Figure 2-Supplement**).

The following videos, illustrating the echocardiographic findings, are available in the on-line supplement:

- 45\_NoPEEP\_ZeroMin.wmv (45/0)
- 45\_NoPEEP\_20Min.wmv (45/0)
- 45\_PlusPEEP\_ZeroMin.wmv (45/10)
- 45\_PlusPEEP\_20Min.wmv (45/10)

**SERIES #4:** Animals were assigned to ventilation groups as in Series #2. The right ventricular peak systolic pressure was less during inspiration than expiration at 0 and 20 min in 45/0, but was not altered by respiration in 45/10 (**Table 2**); specimen traces are provided (**Figure 3-**

KATIRA ET AL

**Supplement**). The (expiratory) RVSP and RVSP-TM progressively decreased in 45/0 during the experiment, but decreased in 45/10 with initial application of PEEP, and stabilized thereafter (**Table 2, Figure 4-B**). RVEDP was lower in 45/0 vs. 45/10 due to the addition of PEEP (10 cmH<sub>2</sub>O) (**Table 2**). The RCPP progressively decreased in 45/0, but was not different from 45/10 at 20 min (**Table 2**). The  $\Delta P_L$  was significantly greater in 45/0 vs. 45/10 (**Table 4-Supplement**).

**SERIES #5:** Animals were assigned to ventilation groups as in Series #2. The LVSP and LVSP-TM progressively decreased in 45/0, but in 45/10 (following initial application of PEEP) remained stable (**Table 5-Supplement**). In 45/0, the LVEDP and mean LVEDP-TM increased progressively, from 9 to 14 mmHg (**Figure 5, Table 5-Supplement**), whereas in 45/10, the LVEDP-TM was lower than in 45/0 through the experiment (**Table 5-Supplement**). Representative traces are provided (**Figure 4-Supplement**).

## DISCUSSION

The current study reproduced the data reported in the classic study by Webb and Tierney (12). The pulmonary edema is due to a large increase in microvascular permeability, as previously shown (7, 8, 16), in addition to a modest ( $\approx 40\%$ ) increase in hydrostatic pressure, which may augment edema formation (18, 28). Ultimately, with high tidal volume and the absence of PEEP, acute *cor pulmonale* develops and is lethal. These effects are in addition to lung inflammation that occurs because of repetitive pulmonary strain.

Several points are important in drawing these conclusions. The original study (12) showed that ventilation with either moderate  $P_{aw}$  (30 cmH<sub>2</sub>O) or high  $P_{aw}$  with PEEP (45/10 cmH<sub>2</sub>O) caused mild injury, but that ventilation with high  $P_{aw}$  and zero PEEP (45/0 cmH<sub>2</sub>O) caused rapid, severe (and lethal) injury (12). These important results were reproduced in the current study (**Series 1**), in terms of lung/body weight ratio (pulmonary edema), histology, mortality, and comparable values for arterial blood gas and dynamic compliance at the beginning and end of the experiment in each group. As previously shown (7, 8, 16), the current study also demonstrated that with 45/0, microvascular permeability is increased (**Series 2, Figure 2**) and the high W/D ratio indicated development of substantial pulmonary edema (**Figure 2-B**).

Additional insight in the present study derives from hemodynamic studies (**Series 3, 4 and 5**). Here, events can be described as those influenced by the respiratory cycle (*i.e.* inspiration vs. expiration), and those that evolved over the course of the experiment (20 mins). In 45/0, echocardiography demonstrated that the end-diastolic RV area (surrogate for end-diastolic RV volume) was reduced during inspiration (**Figures 3, Table 1**); *i.e.*, during inspiration, preload

was reduced with concomitant absence of pulmonary artery flow (**Table 1**). During expiration, filling and stroke volume (SV) were greater (**Figures 3, Table 1**).

The ratio of right ventricular ejection time to pulmonary artery acceleration time (RVET:PAAT; a surrogate of pulmonary vascular resistance, PVR) was high during expiration in 45/0 (**Table 1**; however, during inspiration, it is not reportable because of absent flow). The high inspiratory pressure can compress alveolar capillaries creating zone I and II conditions (29); this could impose a high afterload on the right heart (30). Thus, the right ventricular output and afterload undergo large cyclic swings in 45/0. Lesser degrees of oscillation also occurred in 45/10. Similar effects of differential lung volume on PVR have been shown in canine lobes (31).

The left ventricular (LV) stroke volume (SV) also undergoes cyclic changes with respiration, and the magnitude is similar in 45/10 vs. 45/0 (**Table 1**). It is important to note that in 45/0, during expiration at time = 0 min, the RVSV was transiently greater than the LVSV, suggesting that phasic pooling of blood occurred in the pulmonary circuit. In contrast, in 45/10 the RV and LV stroke volumes were similar.

High-fidelity pressure recording (Millar Catheter, **Series 4**) confirmed that in 45/0 the RVSP reduced significantly during inspiration, concomitant with interruption of flow (*i.e.* absent preload; **Table 2, Figure 3-Supplement**), whereas in 45/10 the RVSP was unchanged.

During mechanical ventilation, changes in pleural ( $P_{pl}$ ) and trans pulmonary pressure ( $P_L$ ) (as well as pulmonary artery and venous pressures, and flow) contribute to pulmonary microvascular hydrostatic pressure ( $P_{mv}$ ) (32). We demonstrated high inspiratory  $P_L$  in 45/0 (**Table 4-Supplement**) and this could potentially obliterate post-capillary venous flow, increasing the local proximal microvascular hydrostatic pressure ( $P_{mv}$ ) (33). Increases in  $P_L$  and

$P_{mv}$  can each cause capillary stretch (34, 35), and could be exacerbated by the expiratory increase in RV SV, especially in Zone II or III conditions. Finally, where expiratory  $P_{aw}$  is zero, the transmural  $P_{mv}$  is high. Taken together, these effects could potentiate capillary wall stress, which in small animals has been described at relatively modest pressure elevations (36). This is consistent with the sequence reported in this model of VILI by Dreyfuss et al (8), where high  $V_T$  injury results in endothelial lesions before epithelial lesions.

The effects of inspiratory swings on  $P_{pl}$  and  $P_L$  have been modeled by computer simulation (32): increases in  $P_{pl}$  primarily reduce RV preload (as we observed; **Figure 3, Table 1**) and changes in  $P_L$  primarily increase RV afterload by development of West's Zone 1 or 2 conditions (i.e., absent or interrupted pulmonary perfusion); these hemodynamic changes were reduced by addition of PEEP (45/10) reflecting the reduced swings in  $P_{pl}$  and  $P_L$  (**Table 4-Supplement**). These marked swings in RV volume and pulmonary perfusion resulted in marked reverse pulsus paradoxus in 45/0 compared to 45/10 (**Figure 3 Supplement**).

In 45/10, with each respiratory cycle the RV area (therefore volume) underwent no change; however, the RV systolic pressure increased and the output fell. These changes may indicate an effect of PEEP on the peripheral circulation (reviewed by Nanas & Magder, 1992)(37).

In 45/0, the RV systolic (and the transmural systolic) pressure fell over the course of the experiment, the RV area increased (**Tables 1, 2; Figure 4**), and TAPSE decreased (**Figure 2-Supplement**), all consistent with acute RV failure. Inspiratory (vs. expiratory) RV volume, 45/0 reflects RV preload (a function of swings in  $P_{pl}$ ), whereas dilation over the course of the experiment reflects increasing afterload (i.e. *cor pulmonale*) (**Table 1**). This was accompanied by decreased LV end-diastolic area, slightly increased LVEDP (i.e. transmural LVEDP, the 'effective'

pressure) (**Figure 5, Figure 4-Supplement**), higher systolic eccentricity index (**Table 1**) and reduced LVSV (**Table 1**). It is important to note here that LVEDP-TM (and not LVEDP) is the effective hydrostatic pressure that best reflects the pulmonary microvascular pressure. It is also important to note that the measures of PVR (*i.e.* RVET/PAAT) are flow-dependent; hence the values are underestimated at 20 min due to RV failure (during expiration, due to insufficient flow) and are not reportable during inspiration (due to absent flow).

The LVEDP-TM is increased in 45/0, and the contributors include compression by the dilated RV (*cor pulmonale*, **Figure 4**) and this parallels increased LV afterload and wall stress (**Figure 5B-Supplement**). Although LVEDP-TM is an underestimation of the pulmonary microvascular hydrostatic pressure ( $P_{mv}$ ) (35, 38), the modest increase in observed  $P_{mv}$  would not cause edema, but in the presence of increased permeability, would exacerbate edema (18, 28).

An important insight may be observed from the hemodynamic changes at the beginning of the experiment. The cardiac output decreased to the same extent in 45/0 and 45/10, but the decrease in mean arterial pressure was greater in 45/10 (**Table 1-Supplement**). Therefore, the systemic vascular (and hence the LV afterload) must have been higher in 45/0; this is reflected in the increased LV systolic transmural pressure (**Figure 5-Supplement**), and this would be associated with an increased propensity to pulmonary edema.

The pathogenesis of pulmonary edema involves factors affecting fluid filtration and the integrity of the microvascular membrane (39). In the context of VILI, a major contributor to edema is microvascular membrane damage from stretch (8); moreover, reducing this stress ( $V_T$ ) reduces edema formation (16, 19). Increased permeability to protein from such microvascular damage has previously been demonstrated in experimental VILI (7, 8), and is recapitulated in

the current study (**Figure 2-A**). Pulmonary edema predominates in regions of increased pulmonary perfusion (38), because increased microvascular pressure augments the rate of edema development in the setting of increased permeability (**Figure 2-A**) as shown previously (18, 28) and can increase permeability (35, 40, 41). Also, higher vascular flows (as seen during expiration in this model) together with increasing microvascular pressure can further enhance edema formation (42). A contribution of microvascular pressures has been reported in isolated perfused (43-46) or open-chested (18) models of VILI, and is consistent with the demonstration in the current model, of increased permeability (**Figure 2-A**), increased microvascular pressure (**Figure 5, Figure 4-Supplement**), and increased overall edema formation (**Figure 1, 2-B**).

The edema in 45/10 is less than in 45/0 (**Figure 1**). Application of PEEP (higher mean  $P_{aw}$ ) may further compress collapsible microvasculature, and reduce cardiac output which may in turn de-recruit the capillary bed; both higher  $P_{aw}$  and lower perfusion may reduce the surface area of perfused capillaries. In addition, with PEEP 10 cmH<sub>2</sub>O, the higher  $P_{aw}$  and the reduced  $P_{mv}$  (**Figure 5**) together decrease transmural  $P_{mv}$ . Together, these factors may contribute to less edema formation in 45/10. Of note, dopamine infusion in this model (45/10) increased edema formation (19), presumably by increasing pulmonary perfusion and/or microvascular pressure.

Of note the RVSV and LVSV are less out of phase (**Table 1**) than would be expected with positive pressure ventilation, because the ratio of heart rate to respiratory rate is high (300/30 = 10 times). Thus, compression and emptying of the RV in this rodent experiment would result in forward emptying of the LV within the same inspiration.

The acute RV dilation (45/0) noted in this study (**Figure 4-A**) represents acute *cor pulmonale* which in turn results from increased pulmonary vascular resistance (PVR). The reasons for

KATIRA ET AL

increased PVR may include high inspiratory airway pressure causing phasic zones of non-perfusion and increased right ventricle afterload (above)(30). However, due to simultaneous volume unloading of the right ventricle, pressure loading could not be contemporaneously accessed. In addition, the absence of PEEP would result in low expiratory lung volume, and could independently increase PVR (47)(**Table 1**, RVET:PAAT ratio). Finally, the development of pulmonary edema and hypoxemia can also increase PVR (although PaCO<sub>2</sub> was not elevated). Pulmonary vascular injury may also have contributed to the increased PVR. There is clear evidence of such injury, such as increased permeability in the current (**Figure 2-A**) and previous (7, 8) studies, and previously reported endothelial lesions (8). It is possible, though not proved, that such injury was caused by the cyclic interruption of pulmonary vascular flow. For example, phasic changes in pulmonary blood flow contribute to lung edema (43), and reperfusion of ischemic lungs can lead to pulmonary microvascular injury (48, 49). Also, repetitive 'stress' is often more injurious than single stressors (50), and this has been conceptually proposed in VILI (38). In addition, changes in flow can increase endothelial permeability *in vitro* (51). Finally, the presence of neutrophil infiltration (**Figure 1-Supplement**) indicates acute inflammation, but the rapid mortality suggests lethal circulatory failure.

There are limitations to the current data. The study was not entirely replicated: groups 30/10 and Control (spontaneously breathing) were omitted because they were not relevant to studying the outcome of interest (**Table 1-Supplement**). Although the original study had more groups (6 vs. 4), the current study was randomized whereas the original was not. The precise processing details of lung histology were uncertain and we performed standardized (20) histologic processing and interpretation that reflect well the original patterns of injury (12)

(**Figure 2; Table 3-supplement**). Additional differences included the use of Hilltop HLA-W rats (200-250 g), and Halothane/Pentobarbital anesthesia (12); in contrast, current experiments employed heavier (300-500 g) Sprague-Dawley rats, and Ketamine/Xylazine anesthesia. Although increased RV afterload is inferred, we did not record increased RV systolic pressure. Finally, while left ventricular pressures and shape were monitored, left ventricular function was not.

In conclusion, this classic work (12), one of the foremost in the field of ventilator-induced lung injury, involves swings in RV filling and stroke volume, acute *cor pulmonale* and a modest increase in LVEDP.

**FIGURE 1 – PULMONARY EDEMA IN CURRENT AND HISTORICAL COMPARISONS (SERIES 1):** The patterns of pulmonary edema (black columns) in **Series 1** are similar to those observed in the historical study by Webb and Tierney (gray columns). Pulmonary edema is the ratio of the wet lung weight to the body weight (expressed as a percentage). The duration of these experiments was 60mins. \*P<0.001, 45/0 vs. other groups (current study data only).

**FIGURE 2 – PERMEABILITY AND LUNG WATER OVER 20 MIN. (SERIES 2):** Permeability to protein (Panel A) and lung water (Panel B) was greater in 45/0 vs. 45/10 in experiments that were terminated at 20 min (**Series 2**). Permeability was determined by absorbance of Evans Blue dye in the bronchoalveolar lavage and lung water was estimated by the lung wet-to-dry weight ratio. \*P<0.05, 45/0 vs. 45/10 (10/3 is for inspection, not included in analysis: n=2).

**FIGURE 3 – VENTRICULAR FILLING DURING INSPIRATION (SERIES 3):** During inspiration there is under-filling and collapse of the right ventricle in the 45/0 group, while chamber volumes are normal in the 45/10 group (video clips are available in the on-line supplement). **Abbreviations:** RV right ventricle; LV left ventricle.

**FIGURE 4 – RIGHT VENTRICULAR SIZE AND SYSTOLIC PRESSURE (SERIES 3 AND 4):** The RV area indexed to the LV (RV:LV Ratio) increased in 45/0 and was unchanged in 45/10 (Panel A). In parallel with the increase in RV size, the RV systolic pressure decreased over time in 45/0, but not in 45/10 (Panel B). All measurements were made in expiration. \*P<0.05, 2-way RM ANOVA. **Abbreviations:** RV right ventricle; LV left ventricle; RVSP right ventricular systolic pressure.

**FIGURE 5 – LEFT VENTRICULAR END-DIASTOLIC PRESSURE (SERIES 5):** The transmural left ventricular end-diastolic pressure increased significantly during the experiment in 45/0, but the values were lower in 45/10. \*P<0.05, 2-way RM ANOVA. **Abbreviations:** LVEDP-TM Transmural left ventricular end-diastolic pressure.

## REFERENCES

## References

1. Amato MB, Barbas CS, Medeiros DM, Magaldi RB, Schettino GP, Lorenzi-Filho G, Kairalla RA, Deheinzelin D, Munoz C, Oliveira R, Takagaki TY, Carvalho CR. Effect of a protective-ventilation strategy on mortality in the acute respiratory distress syndrome. *N Engl J Med* 1998;338:347-354.
2. Ventilation with lower tidal volumes as compared with traditional tidal volumes for acute lung injury and the acute respiratory distress syndrome. The acute respiratory distress syndrome network. *N Engl J Med* 2000;342:1301-1308.
3. Hickling KG, Henderson SJ, Jackson R. Low mortality associated with low volume pressure limited ventilation with permissive hypercapnia in severe adult respiratory distress syndrome. *Intensive Care Med* 1990;16:372-377.
4. Hickling KG, Walsh J, Henderson S, Jackson R. Low mortality rate in adult respiratory distress syndrome using low-volume, pressure-limited ventilation with permissive hypercapnia: A prospective study. *Crit Care Med* 1994;22:1568-1578.
5. Lachmann B, Jonson B, Lindroth M, Robertson B. Modes of artificial ventilation in severe respiratory distress syndrome. Lung function and morphology in rabbits after wash-out of alveolar surfactant. *Crit Care Med* 1982;10:724-732.
6. Hamilton PP, Onayemi A, Smyth JA, Gillan JE, Cutz E, Froese AB, Bryan AC. Comparison of conventional and high-frequency ventilation: Oxygenation and lung pathology. *J Appl Physiol Respir Environ Exerc Physiol* 1983;55:131-138.
7. Parker JC, Townsley MI, Rippe B, Taylor AE, Thigpen J. Increased microvascular permeability in dog lungs due to high peak airway pressures. *J Appl Physiol Respir Environ Exerc Physiol* 1984;57:1809-1816.
8. Dreyfuss D, Basset G, Soler P, Saumon G. Intermittent positive-pressure hyperventilation with high inflation pressures produces pulmonary microvascular injury in rats. *Am Rev Respir Dis* 1985;132:880-884.
9. Dreyfuss D, Saumon G. Ventilator-induced lung injury: Lessons from experimental studies. *Am J Respir Crit Care Med* 1998;157:294-323.
10. Greenfield LJ, Ebert PA, Benson DW. Effect of positive pressure ventilation on surface tension properties of lung extracts. *Anesthesiology* 1964;25:312-316.
11. Faridy EE, Permutt S, Riley RL. Effect of ventilation on surface forces in excised dogs' lungs. *J Appl Physiol* 1966;21:1453-1462.
12. Webb HH, Tierney DF. Experimental pulmonary edema due to intermittent positive pressure ventilation with high inflation pressures. Protection by positive end-expiratory pressure. *Am Rev Respir Dis* 1974;110:556-565.
13. Egan EA, Nelson RM, Olver RE. Lung inflation and alveolar permeability to non-electrolytes in the adult sheep in vivo. *J Physiol* 1976;260:409-424.
14. Egan EA. Response of alveolar epithelial solute permeability to changes in lung inflation. *J Appl Physiol Respir Environ Exerc Physiol* 1980;49:1032-1036.
15. Egan EA. Lung inflation, lung solute permeability, and alveolar edema. *J Appl Physiol Respir Environ Exerc Physiol* 1982;53:121-125.
16. Dreyfuss D, Soler P, Basset G, Saumon G. High inflation pressure pulmonary edema. Respective effects of high airway pressure, high tidal volume, and positive end-expiratory pressure. *Am Rev Respir Dis* 1988;137:1159-1164.
17. Hernandez LA, Peevy KJ, Moise AA, Parker JC. Chest wall restriction limits high airway pressure-induced lung injury in young rabbits. *J Appl Physiol (1985)* 1989;66:2364-2368.

18. Parker JC, Hernandez LA, Longenecker GL, Peevy K, Johnson W. Lung edema caused by high peak inspiratory pressures in dogs. Role of increased microvascular filtration pressure and permeability. *Am Rev Respir Dis* 1990;142:321-328.
19. Dreyfuss D, Saumon G. Role of tidal volume, frc, and end-inspiratory volume in the development of pulmonary edema following mechanical ventilation. *Am Rev Respir Dis* 1993;148:1194-1203.
20. Tsuchida S, Engelberts D, Peltekova V, Hopkins N, Frndova H, Babyn P, McKelrie C, Post M, McLoughlin P, Kavanagh BP. Atelectasis causes alveolar injury in nonatelectatic lung regions. *Am J Respir Crit Care Med* 2006;174:279-289.
21. Verbrugge SJ, Vazquez de Anda G, Gommers D, Neggers SJ, Sorm V, Bohm SH, Lachmann B. Exogenous surfactant preserves lung function and reduces alveolar Evans blue dye influx in a rat model of ventilation-induced lung injury. *Anesthesiology* 1998;89:467-474.
22. Liu J, Rigel DF. Echocardiographic examination in rats and mice. *Methods Mol Biol* 2009;573:139-155.
23. Slama M, Susic D, Varagic J, Ahn J, Frohlich ED. Echocardiographic measurement of cardiac output in rats. *Am J Physiol Heart Circ Physiol* 2003;284:H691-697.
24. Ryan T, Petrovic O, Dillon JC, Feigenbaum H, Conley MJ, Armstrong WF. An echocardiographic index for separation of right ventricular volume and pressure overload. *J Am Coll Cardiol* 1985;5:918-927.
25. Kimura K, Daimon M, Morita H, Kawata T, Nakao T, Okano T, Lee SL, Takenaka K, Nagai R, Yatomi Y, Komuro I. Evaluation of right ventricle by speckle tracking and conventional echocardiography in rats with right ventricular heart failure. *Int Heart J* 2015;56:349-353.
26. Lai YL, Hildebrandt J. Respiratory mechanics in the anesthetized rat. *J Appl Physiol Respir Environ Exerc Physiol* 1978;45:255-260.
27. Cross CE. Right ventricular pressure and coronary flow. *Am J Physiol* 1962;202:12-16.
28. Huchon GJ, Hopewell PC, Murray JF. Interactions between permeability and hydrostatic pressure in perfused dogs' lungs. *J Appl Physiol Respir Environ Exerc Physiol* 1981;50:905-911.
29. West JB, Dollery CT, Naimark A. Distribution of blood flow in isolated lung; relation to vascular and alveolar pressures. *J Appl Physiol* 1964;19:713-724.
30. Permutt S, Bromberger-Barnea B, Bane HN. Alveolar pressure, pulmonary venous pressure, and the vascular waterfall. *Med Thorac* 1962;19:239-260.
31. Creamer KM, McCloud LL, Fisher LE, Ehrhart IC. Ventilation above closing volume reduces pulmonary vascular resistance hysteresis. *Am J Respir Crit Care Med* 1998;158:1114-1119.
32. Magder S, Guerard B. Heart-lung interactions and pulmonary buffering: Lessons from a computational modeling study. *Respir Physiol Neurobiol* 2012;182:60-70.
33. Lopez-Muniz R, Stephens NL, Bromberger-Barnea B, Permutt S, Riley RL. Critical closure of pulmonary vessels analyzed in terms of Starling resistor model. *J Appl Physiol* 1968;24:625-635.
34. Fu Z, Costello ML, Tsukimoto K, Prediletto R, Elliott AR, Mathieu-Costello O, West JB. High lung volume increases stress failure in pulmonary capillaries. *J Appl Physiol (1985)* 1992;73:123-133.
35. West JB, Tsukimoto K, Mathieu-Costello O, Prediletto R. Stress failure in pulmonary capillaries. *J Appl Physiol (1985)* 1991;70:1731-1742.
36. KM W. Effects of pressure and flow on pulmonary endothelium. In: Norbert VF RS, editor. The pulmonary endothelium: Function in health and disease: John Wiley & Sons, Ltd; 2009.
37. Nanas S, Magder S. Adaptations of the peripheral circulation to PEEP. *Am Rev Respir Dis* 1992;146:688-693.
38. Marini JJ, Hotchkiss JR, Broccard AF. Bench-to-bedside review: Microvascular and airspace linkage in ventilator-induced lung injury. *Crit Care* 2003;7:435-444.
39. Staub NC. "State of the art" review. Pathogenesis of pulmonary edema. *Am Rev Respir Dis* 1974;109:358-372.

40. Yin J, Hoffmann J, Kaestle SM, Neye N, Wang L, Baeurle J, Liedtke W, Wu S, Kuppe H, Pries AR, Kuebler WM. Negative-feedback loop attenuates hydrostatic lung edema via a cgmp-dependent regulation of transient receptor potential vanilloid 4. *Circ Res* 2008;102:966-974.
41. Jian MY, King JA, Al-Mehdi AB, Liedtke W, Townsley MI. High vascular pressure-induced lung injury requires p450 epoxigenase-dependent activation of trpv4. *Am J Respir Cell Mol Biol* 2008;38:386-392.
42. Lopez-Aguilar J, Piacentini E, Villagra A, Murias G, Pascotto S, Saenz-Valiente A, Fernandez-Segoviano P, Hotchkiss JR, Blanch L. Contributions of vascular flow and pulmonary capillary pressure to ventilator-induced lung injury. *Crit Care Med* 2006;34:1106-1112.
43. Hotchkiss JR, Jr., Blanch L, Naveira A, Adams AB, Carter C, Olson DA, Leo PH, Marini JJ. Relative roles of vascular and airspace pressures in ventilator-induced lung injury. *Crit Care Med* 2001;29:1593-1598.
44. Broccard AF, Hotchkiss JR, Kuwayama N, Olson DA, Jamal S, Wangenstein DO, Marini JJ. Consequences of vascular flow on lung injury induced by mechanical ventilation. *Am J Respir Crit Care Med* 1998;157:1935-1942.
45. Broccard AF, Hotchkiss JR, Suzuki S, Olson D, Marini JJ. Effects of mean airway pressure and tidal excursion on lung injury induced by mechanical ventilation in an isolated perfused rabbit lung model. *Crit Care Med* 1999;27:1533-1541.
46. Hotchkiss JR, Jr., Blanch L, Murias G, Adams AB, Olson DA, Wangenstein OD, Leo PH, Marini JJ. Effects of decreased respiratory frequency on ventilator-induced lung injury. *Am J Respir Crit Care Med* 2000;161:463-468.
47. Whittenberger JL, Mc GM, Berglund E, Borst HG. Influence of state of inflation of the lung on pulmonary vascular resistance. *J Appl Physiol* 1960;15:878-882.
48. Pierre AF, DeCampos KN, Liu M, Edwards V, Cutz E, Slutsky AS, Keshavjee SH. Rapid reperfusion causes stress failure in ischemic rat lungs. *J Thorac Cardiovasc Surg* 1998;116:932-942.
49. Atochina EN, Muzykantov VR, Al-Mehdi AB, Danilov SM, Fisher AB. Normoxic lung ischemia/reperfusion accelerates shedding of angiotensin converting enzyme from the pulmonary endothelium. *Am J Respir Crit Care Med* 1997;156:1114-1119.
50. Hashin Z, Rotem A. A cumulative damage theory of fatigue failure. *Materials Science and Engineering* 1978;34:147-160.
51. Jo H, Dull RO, Hollis TM, Tarbell JM. Endothelial albumin permeability is shear dependent, time dependent, and reversible. *Am J Physiol* 1991;260:H1992-1996.

**Table 1 – Echocardiographic Variables (*Series 3*)**

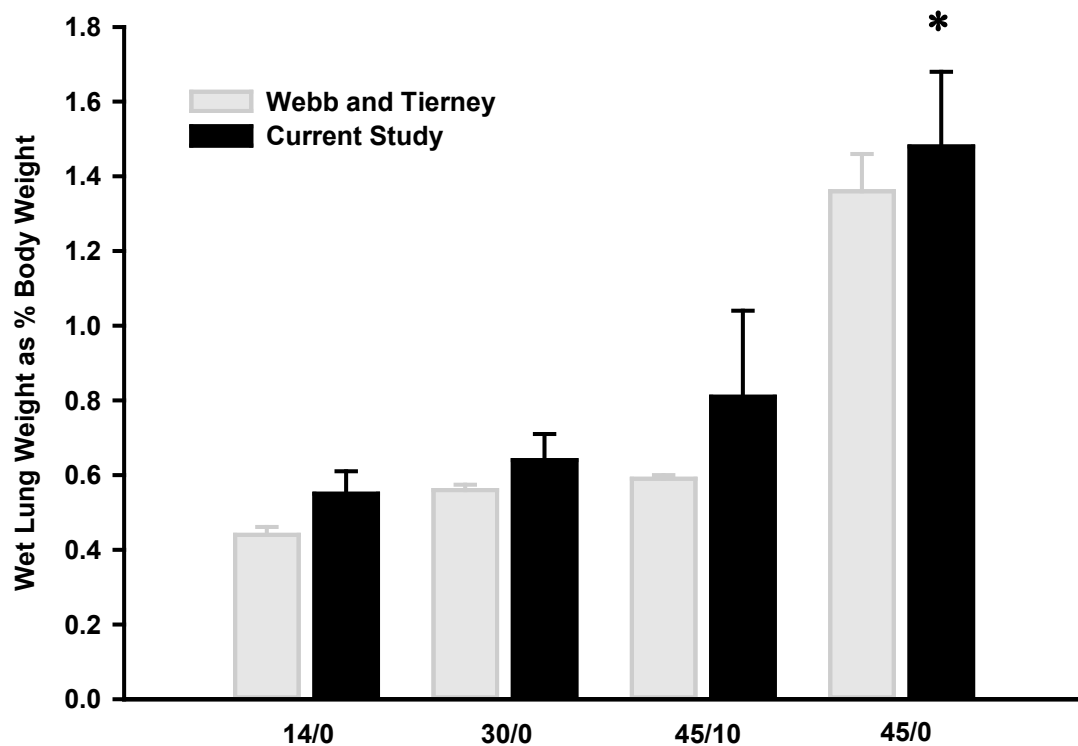
	45/0 (n = 4)			45/10 (n = 4)		
	Baseline	0 min	20 min	Baseline	0 min	20 min
<b>RV Area Inspiration</b>	0.07±0.02	0.0 <sup>‡</sup>	0.13±0.26 <sup>‡</sup>	0.08±0.03	0.16±0.06	0.16±0.06
<b>RV Area Expiration</b>	0.07±0.02	0.20±0.06	0.55±0.12 <sup>**</sup>	0.08±0.03	0.16±0.11	0.21±0.10
<b>LV Area Inspiration</b>	0.48±0.07	0.24±0.02 <sup>‡</sup>	0.21±0.11 <sup>†‡</sup>	0.42±0.07	0.34±0.02	0.36±0.12
<b>LV Area Expiration</b>	0.48±0.07	0.37±0.11	0.30±0.06	0.42±0.07	0.36±0.06	0.40±0.11
<b>RV:LV Ratio Inspiration</b>	0.15±0.07	0.00±0.0	1.63±3.3	0.18±0.04	0.43±0.2	0.45±0.09
<b>RV:LV Ratio Expiration</b>	0.15±0.07	0.61±0.36	1.9±0.6 <sup>**</sup>	0.18±0.04	0.43±0.23	0.52±0.12
<b>RV SV Inspiration</b>	0.48±0.15	0.07±0.13 <sup>‡</sup>	0.0±0.0 <sup>†‡</sup>	0.45±0.1	0.16±0.03 <sup>‡</sup>	0.15±0.07 <sup>‡</sup>
<b>RV SV Expiration</b>	0.61±0.1	0.8±0.17 <sup>†</sup>	0.44±0.15 <sup>*</sup>	0.57±0.04	0.55±0.08	0.51±0.07
<b>LV SV Inspiration</b>	0.47±0.1	0.23±0.07 <sup>‡</sup>	0.11±0.13 <sup>*†‡</sup>	0.42±0.07	0.26±0.05 <sup>‡</sup>	0.27±0.06 <sup>‡</sup>
<b>LV SV Expiration</b>	0.59±0.15	0.51±0.16	0.36±0.17	0.55±0.1	0.47±0.1	0.52±0.05
<b>RVET:PAAT Inspiration</b>	2.67±0.23	--	--	2.75±0.49	2.68±0.39	3.12±1.1
<b>RVET:PAAT Expiration</b>	2.67±0.23	3.9±0.63	3.28±0.68	2.75±0.49	2.8±0.48	2.92±0.47
<b>Eccentricity Diastole</b>	1.03±0.04	1.2±0.27	1.55±0.27	0.96±0.16	1.27±0.13	1.35±0.16
<b>Eccentricity Systole</b>	1.09±0.15	1.27±0.4	2.98±0.75 <sup>**</sup>	1.04±0.41	1.48±0.35	1.69±0.30
<b>Fractional Shortening</b>	52.8±3.9	45.5±3.8	41.6±4.3	49.4±2.1	44.0±1.4	41.3±4.7

Right and Left ventricular area, ratio of right to left ventricular area, stroke volume, and ratio of (RV ejection/PA acceleration) time were measured during inspiration and expiration. Eccentricity of LV in systole and diastole, and fractional shortening, was also recorded. All experiments were terminated at 20 min. Experimental groups were (Peak Airway Pressure/Positive End-Expiratory Pressure): 45/0 and 45/10. Baseline measurements were made before randomization. Statistical Comparisons: <sup>\*</sup>P<0.05 vs. 0 min; <sup>†</sup>P<0.05 vs. 45/10; <sup>‡</sup>P<0.05 vs. expiration. **Abbreviations:** RV *Right Ventricle*; LV *Left ventricle*; Area ( $\text{cm}^2$ ); SV *Stroke Volume (mL/kg)*; RVET *Right Ventricular Ejection Time*; PAAT *Pulmonary Artery Acceleration Time*.

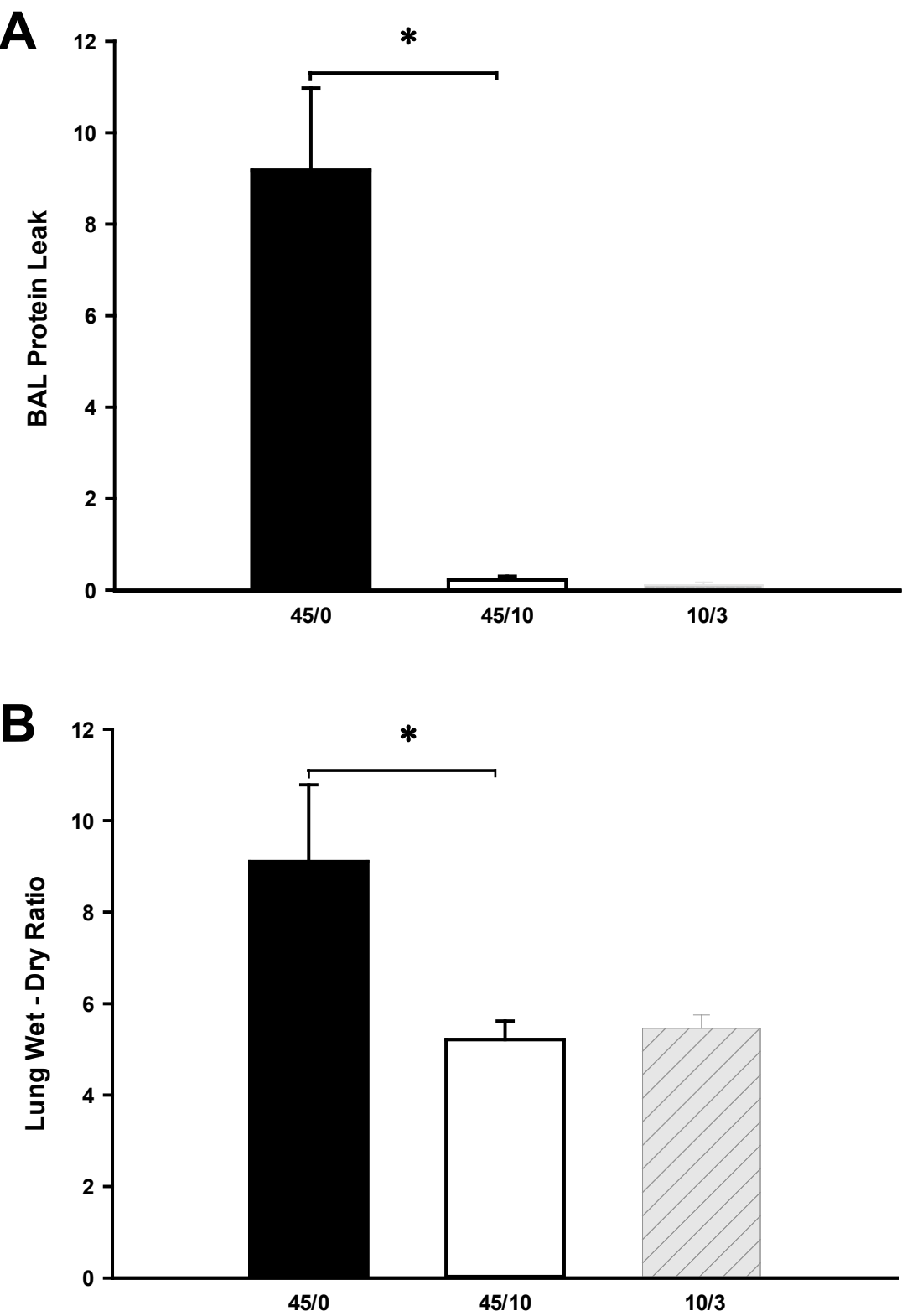
**Table 2 – Hemodynamics during Right Ventricular Pressure Measurement (*Series 4*)**

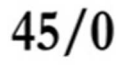
	45/0 (n = 5)			45/10 (n = 5)			10/3 (n = 2)		
	Baseline	0 min	20 min	Baseline	0 min	20 min	Baseline	0 min	20 min
<b>RVSP Inspiration</b>	41.0±20.4	13.2±7.8 <sup>†</sup>	13.8±7.7 <sup>*†</sup>	28.0±11.9	27.9±12.2	27.4±14.6	28.1±5.2	29.2±3.3	34.2±1.8
<b>RVSP Expiration</b>	42.0±18.9	37.4±18.1	24.1±12.0	26.4±11.4	25.3±6	24.8±11.6	28.2±2.5	28.7±1.3	34.8±2.5
<b>RVSP-TM Inspiration</b>	36.5±22.4	8.2±8.5 <sup>†</sup>	9.7±9.5 <sup>†</sup>	27.6±7.5	22±10.6	21.8±13.8	24.5±4.9	25.4±4.0	30.3±1.8
<b>RVSP-TM Expiration</b>	38.0±21.3	34.5±19.4	21.0±13.1	26.5±7.7	21.1±5.1	21.1±10.7	25.3±3.0	25.8±1.6	32.2±2.4
<b>RVEDP Inspiration</b>	3.2±3.7	2.7±4.0	3.4±4.8	5.0±3.0	7.6±2.6	8.4±5.1	3.2±0.1	3.8±0.14	3.3±1.3
<b>RVEDP Expiration</b>	3.4±3.2	2.9±3.8	2.6±4.9 <sup>*</sup>	4.1±3.0	6.1±3.0	7.7±3.7	2.4±0.5	2.8±1.3	2.7±0.8
<b>RVEDP-TM Inspiration</b>	-0.94±5.4	-1.5±5.4	-0.84±6.7	0.88±1.7	1.6±3.1	3.1±4.7	-0.85±0.5	-0.15±0.6	-0.4±0.7
<b>RVEDP-TM Expiration</b>	-0.36±5.2	0.16±5.4	-0.4±6.5	0.53±1.3	2.1±2.8	3.9±3.2	-0.5±0.0	-0.05±0.5	0.4±0.2
<b>MAP</b>	104±17.2	89±22.8	45.5±14.2	74.4±26.1	55.5±9.2	48±8.2	102±9	100±8	60±2.1
<b>Mean RVP</b>	16.2±8.4	12.2±5.1	9.3±4.5 <sup>*</sup>	12.2±4.7	12.6±3.6	13.7±6.1	11.0±0.5	11.3±1	12.7±1.4
<b>Right CPP</b>	87.6±21.8	77±20.4	33±12.2	62.2±28.7	42.8±11.3	34±11.8	91.3±9.4	88±7.1	47±0.7

Right ventricular pressure, systemic arterial pressure and right coronary perfusion pressure at the start and end of all experiments. All experiments were terminated at 20 min. Statistical Comparisons: between-group comparisons are between 45/0 vs. 45/10 only (10/3, are control experiments for inspection; n=2). \*P<0.05 ANOVA (Group x Time); †P<0.05 vs. expiration. **Abbreviations:** RVSP *Right Ventricular Systolic Pressure (mmHg)*; RVSP-TM *Transmural Right Ventricular Systolic Pressure (mmHg)*; RVEDP *Right Ventricular End-Diastolic Pressure (mmHg)*; RVEDP-TM *Transmural Right Ventricular End-Diastolic Pressure (mmHg)*; MAP *Mean Systemic Arterial Pressure (mmHg)*; RVP *Right Ventricular Pressure (mmHg)*; Right CPP *Right Coronary Perfusion Pressure (mmHg)*.

**FIGURE 1 – PULMONARY EDEMA IN CURRENT AND HISTORICAL COMPARISONS (*SERIES 1*):**

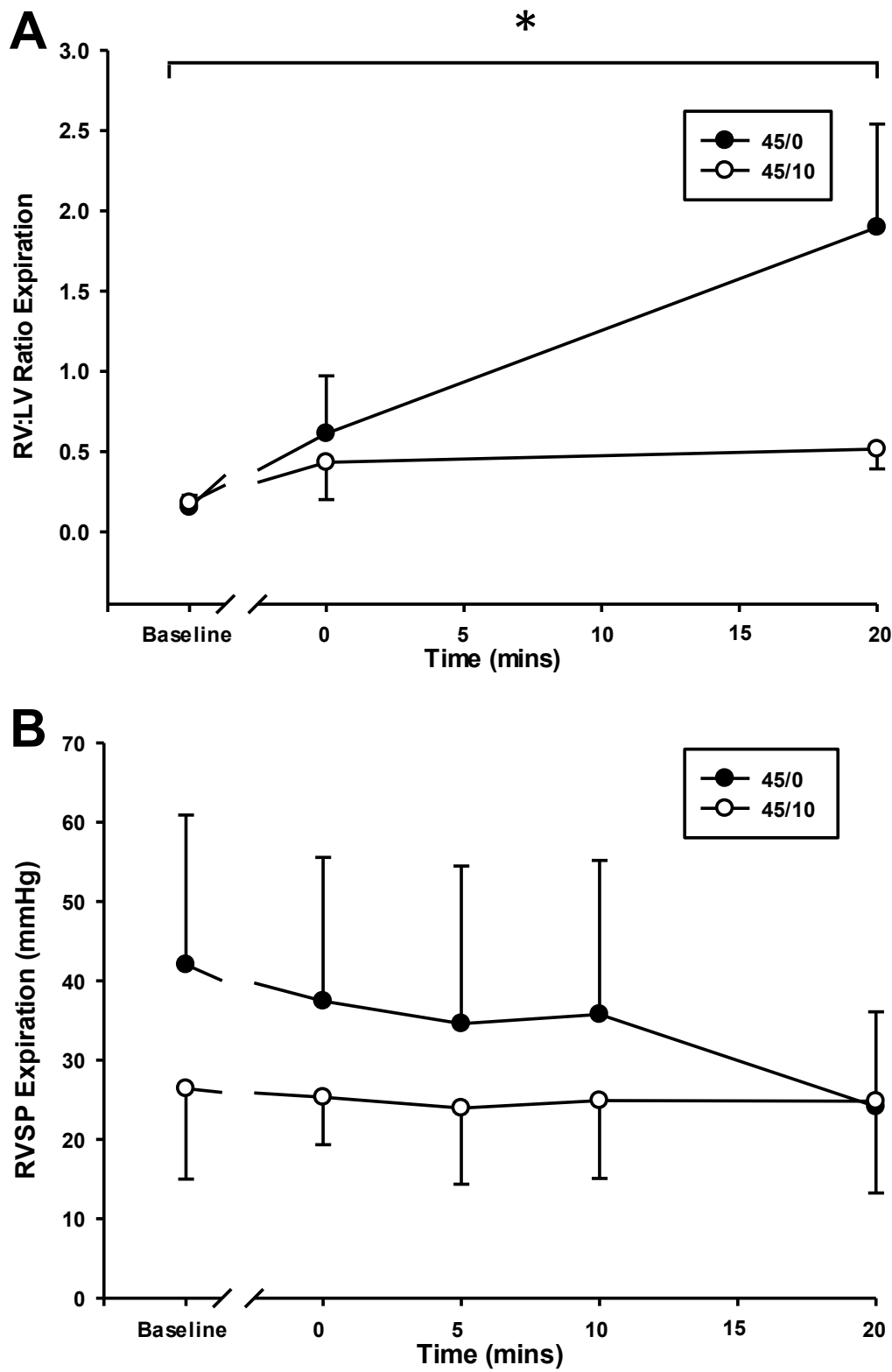
**FIGURE 2 – PERMEABILITY AND LUNG WATER OVER 20 MIN. (SERIES 2):**

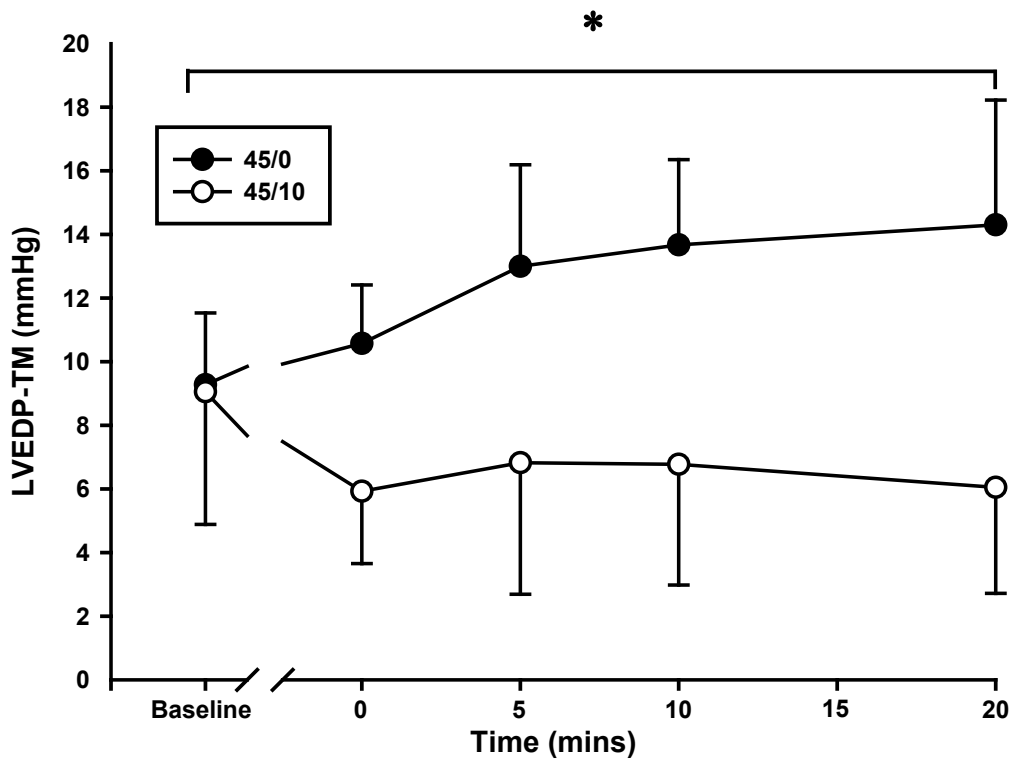




212x164mm (72 x 72 DPI)

FIGURE 4 – RIGHT VENTRICULAR SIZE AND SYSTOLIC PRESSURE (SERIES 3 AND 4):



**FIGURE 5 – LEFT VENTRICULAR END-DIASTOLIC PRESSURE (*SERIES 5*):**

**Video 1 - 45 PlusPEEP ZeroMin (Series 3):**

Ventilation with Paw 45/10 at zero min. - inspiration is associated with minimal change in RV size.

**Video 2 - 45 PlusPEEP 20Min (Series 3):**

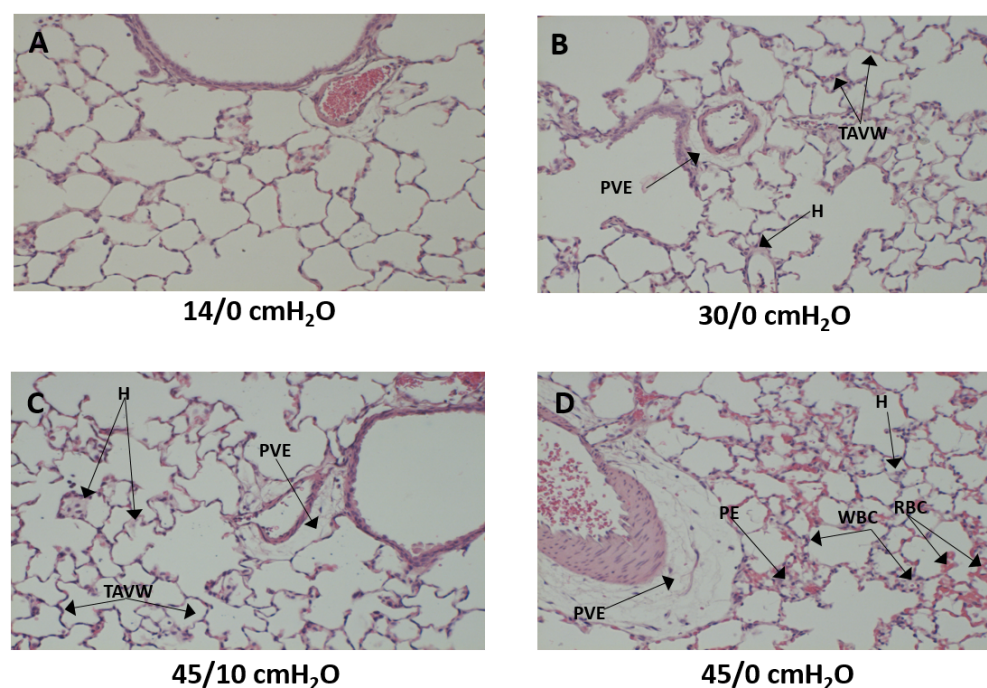
Ventilation with Paw 45/10 at 20 min. - inspiration is associated with minimal change in RV size (similar to zero min, Video 1).

**Video 3 - 45 NoPEEP ZeroMin (Series 3):**

Ventilation with Paw 45/0 at zero min. - inspiration is associated with obliteration of the RV cavity.

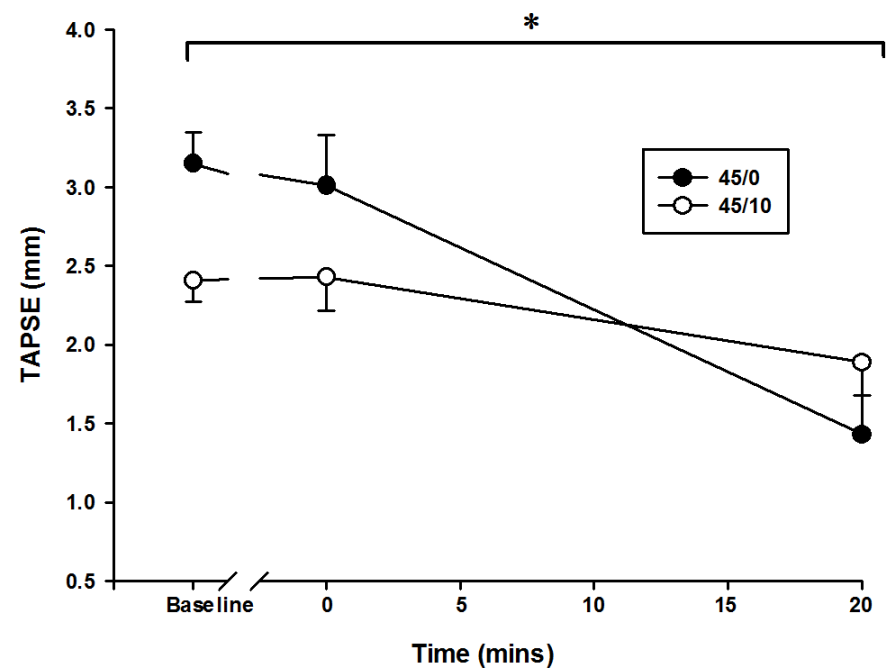
**Video 4 - 45 NoPEEP 20Min (Series 3):**

Ventilation with Paw 45/0 at 20 min. - inspiration is associated with obliteration of the RV cavity, but (in contrast to zero min, Video 3) the RV size in expiration is enlarged.

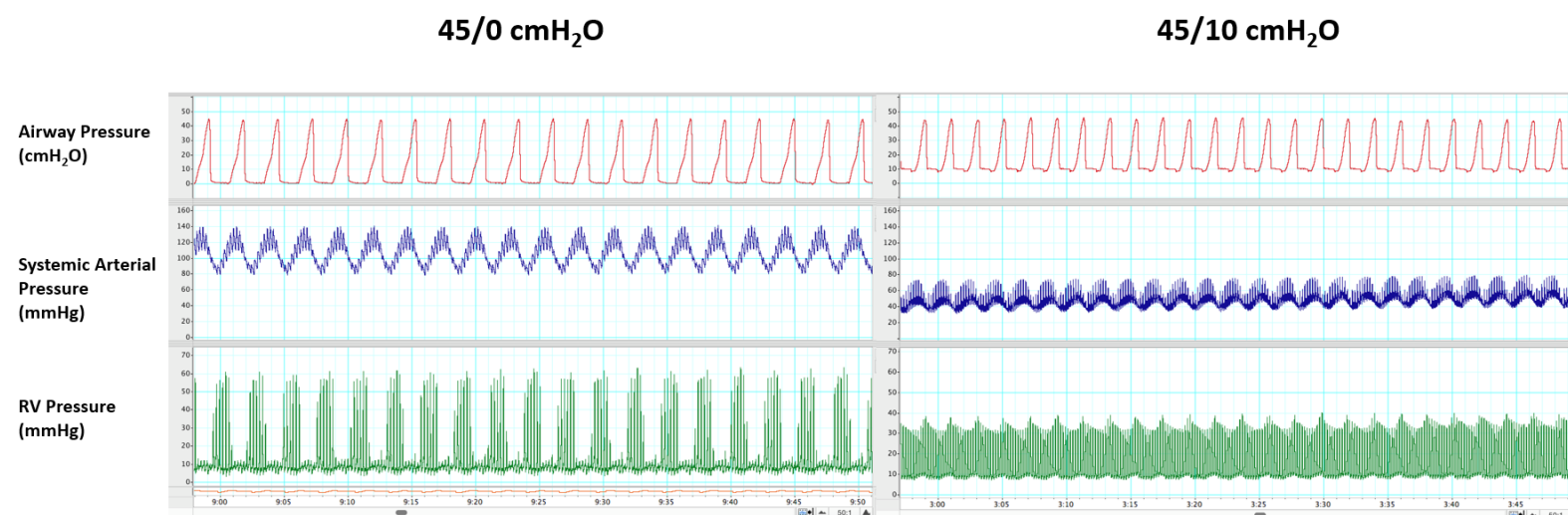
**FIGURE 1 SUPPLEMENT – LUNG HISTOLOGY FOLLOWING MECHANICAL VENTILATION (SERIES 1):**

**Fig. 1 Supplement:** After experiments the lungs were pressure-fixed (10% buffered formalin, 25 cmH<sub>2</sub>O), stained H & E and are imaged at x100. Control ventilation (14/0 cmH<sub>2</sub>O; **Panel A**) shows essentially a normal lung with thin alveolar wall, no cell infiltration and minimal perivascular edema and hyaline membrane. Ventilation with intermediate ‘injury’ ventilation (30/0 cmH<sub>2</sub>O, **Panel B**; 45/10 cmH<sub>2</sub>O, **Panel C**) shows slight thickening of alveolar wall, moderate perivascular edema and hyaline membrane formation. In contrast, injurious ventilation (45/0 cmH<sub>2</sub>O, **Panel D**) shows extensive neutrophil infiltration, hemorrhage, alveolar and perivascular edema, and hyaline membrane formation. **Abbreviations:** TAVW Thickened Alveolar Wall, PVE Perivascular Edema, H Hyaline membrane, WBC White Blood Cells, RBC Red Blood Cells.

**FIGURE 2 SUPPLEMENT – GLOBAL RIGHT VENTRICULAR FUNCTION (SERIES 3):**

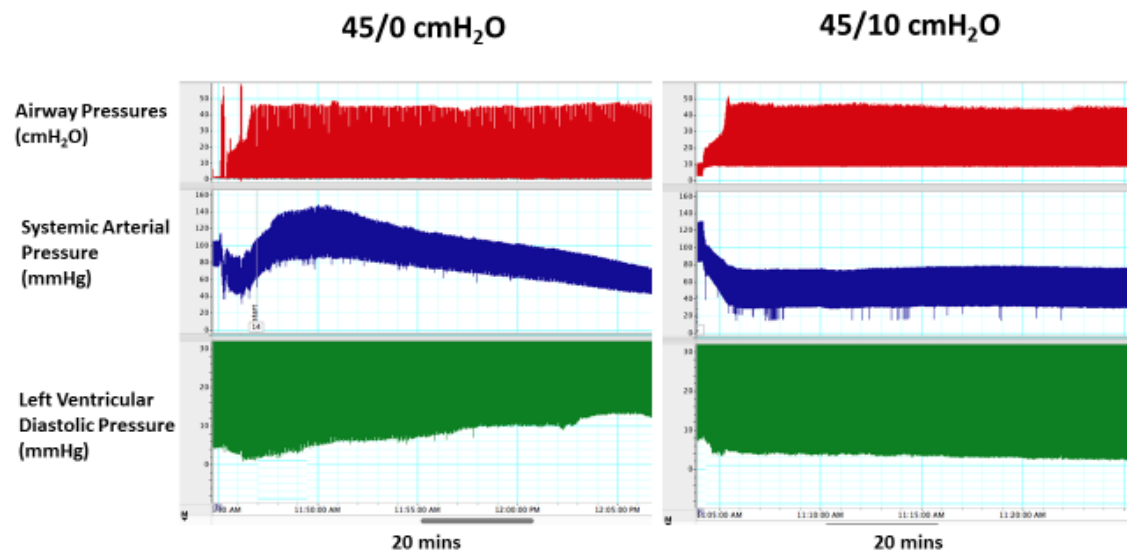


**Fig. 2 Supplement:** The global right ventricular function measured as TAPSE declined progressively in both groups, but to a greater extent in 45/0 than in 45/10. \*P<0.05, 2-way RM ANOVA. **Abbreviations:** TAPSE Tricuspid Annular Plane Systolic Excursion.

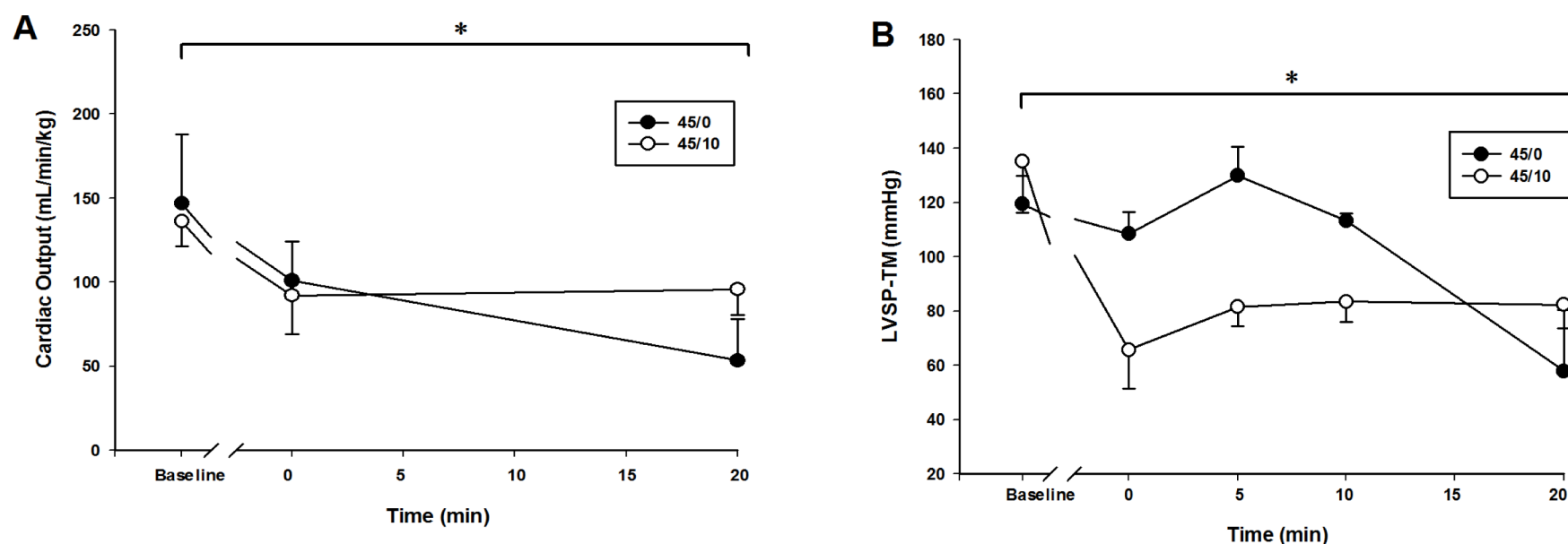
**FIGURE 3 SUPPLEMENT - HIGH FIDELITY RIGHT VENTRICULAR PRESSURE TRACING (SERIES 4):**

**Fig. 3 Supplement:** Representative traces of airway pressure, systemic arterial pressure and right ventricular systolic pressure (high fidelity, Millar Catheter) are shown. Right ventricular systolic pressure decreased during inspiration (see corresponding Airway Pressure) in 45/0 but remained unchanged in 45/10.

**FIGURE 4 SUPPLEMENT – HIGH FIDELITY LEFT VENTRICULAR DIASTOLIC PRESSURE TRACING (SERIES 5):**



**Fig. 4 Supplement:** Representative traces of airway pressure, systemic arterial pressure and left ventricular diastolic pressure (high fidelity, Millar Catheter) are shown. The left ventricular diastolic pressure increased during the experiment in 45/0 but not in 45/10.

**FIGURE 5 SUPPLEMENT – LEFT VENTRICULAR OUTPUT AND AFTERLOAD (SERIES 3 AND 5):**

**Fig. 5 Supplement:** **A)** Left ventricular output decreases similarly in both at the beginning of experiment but progressively declines in 45/0 compared to 45/10. **B)** The Left ventricular afterload (LVSP-TM) increases initially in 45/0 and declines progressively after 10min, whereas in 45/10 after an initial decrease it stays stable. \* $P < 0.05$ , 2-way RM ANOVA. **Abbreviations:** LVSP-TM Left ventricular systolic transmural pressure.

**Table 1 Supplement: Physiologic Parameters (Series 1)**

	14/0 (n = 5)			30/0 (n = 5)			45/0 (n = 5)			45/10 (n = 5)		
	Baseline	0 min	60 min	Baseline	0 min	60 min	Baseline	0 min	Final	Baseline	0 min	60 min
Mean P <sub>AW</sub>	3.8±0.5	4.9±0.8	4.6±0.8	4.2±0.5	7.6±1.2	8.2±1	4.0±0	6.5±0.7	9.1±2	4.0±0	17±0.8	17.3±0.7
V <sub>T</sub>	6	11.6±2.3	11±3.1	6	22.4±1.2	21.7±2.6	6	40.1±3.6	31.5±2.8 <sup>*†</sup>	6	12.2±0.9	12.8±0.6
P <sub>Insp</sub>	7	14	14	7	30	30	7	45	45	7	35	35
C <sub>Dyn</sub>	0.4±0.0	0.4±0.1	0.38±0.1	0.4±0.0	0.37±0.0	0.35±0.0	0.3±0.0	0.3±0.0	0.23±0.0 <sup>*</sup>	0.3±0.0	0.13±0.0	0.13±0.0
RR	60	40	40	60	30	30	60	23	23	60	30	30
I:E ratio	1:1	1:1	1:1	1:1	1:1	1:1	1:1	1:1	1:1	1:1	1:1	1:1
MAP	141±16	123±22	106±13	127±29	137±7.2	119±24	116±26	95±8.7	26±6.5 <sup>*†</sup>	108±24	51.5±1.3	65±23
pH	7.34±0.0	7.35±0.0	7.36±0.1	7.28±0	7.31±0.0	7.30±0.0	7.39±0	7.30±0.0	7.30±0.1	7.28±0	7.30±0.0	7.25±0.0
PaO <sub>2</sub>	97±8.8	97±5.2	71±6.5	93±10	89±9.2	81±7.5	77±3.2	81±6.9	52±8.5 <sup>*†</sup>	79±10	80±7.7	107±5.8
PaCO <sub>2</sub>	38±4	35.7±3.8	34±6.7	43±4.2	39.2±5.5	39±2.4	43±4.6	44±4	35±5.6	44±4	44±3.8	39±3.8
Weight	480±30			490±50			330±30			360±30		

Ventilator parameters, arterial blood pressure and arterial blood gases at the start and end of each experiment. In 14/0, 30/0 and 45/10, all experiments were of 60 min duration; in 45/0, the duration was shorter (mean 26 min, range 18-32 min). Experimental groups were (Peak Airway Pressure/Positive End-Expiratory Pressure): 14/0, 30/0, 45/0 and 45/10. Baseline measurements were made before randomization. Statistical Comparisons: <sup>\*</sup>P<0.05 vs. 0 min; <sup>†</sup>P<0.05 vs. all other groups. **Abbreviations:** P<sub>AW</sub> Airway Pressure (cmH<sub>2</sub>O); V<sub>T</sub> Tidal Volume (mL/kg); P<sub>Insp</sub> Inspiratory Pressure (cmH<sub>2</sub>O); C<sub>Dyn</sub> Dynamic Compliance (mL/cmH<sub>2</sub>O); RR Respiratory Rate; I:E Inspiration: Expiration Ratio; MAP Mean Arterial Pressure (mmHg); pH Arterial pH; PaO<sub>2</sub> Arterial PO<sub>2</sub> (mmHg); PaCO<sub>2</sub> Arterial PCO<sub>2</sub> (mmHg); Weight (gm)

**Table 2 Supplement: Comparison of Histology in W&T and Current Study (Series 1)**

Groups	Webb & Tierney (1974)						Current Study					
	Perivascular Edema					AVE	Perivascular Edema					AVE
	0	1+	2+	3+	4+		0	1+	2+	3+	4+	
<b>14/0</b>	3/6	3/6					5/10	5/10	0/10			
							3/10	6/10	1/10			
<b>30/0</b>			3/5	2/5			0/10	1/10	8/10	1/10		
							5/10	5/10	0/10	0/10		
<b>30/10</b>			4/5	1/5			-	-	-	-	-	-
<b>45/10</b>				4/5	1/5		5/10	5/10	0/10	0/10		
							0/10	4/10	5/10	1/10		
<b>45/0</b>				2/6	4/6	6/6			3/10	7/10	0/10	present
									5/10	4/10	1/10	

Experimental groups included (Peak Airway Pressure/Positive End-Expiratory Pressure): 14/0, 30/0, 30/10, 45/10 and 45/0. The two sets of Data sets in the current study indicate 2 animals in each group with 10 fields studied in each. **Abbreviation:** AVE Alveolar Edema.

Table 3 Supplement – Physiologic Parameters (Series 2)

Variable	45/0 (n = 4)			45/10 (n = 4)			10/3 (n = 2)		
	Baseline	0 min	20 min	Baseline	0 min	20 min	Baseline	0 min	20 min
Mean P <sub>AW</sub>	5.2±0.7	11±0.7	13.9±0.5 <sup>*†</sup>	5.2±0.4	18±0.3	17±0.4	5±0.8	5±0.8	5±0.1
V <sub>T</sub>	6	41.7±1.2	31.4±2.3 <sup>*†</sup>	6	16.2±1.1	16±0.8	6	7.6±0.3	6.5±0.3
P <sub>Insp</sub>	7	45	45	7	35	35	7	7	7
C <sub>Dyn</sub>	0.30±0.0	0.32±0.02	0.24±0.03 <sup>*†</sup>	0.28±0.0	0.15±0.05	0.15±0.01	0.27±0.0	0.3±0.03	0.29±0
I:E ratio	1:1	1:1	1:1	1:1	1:1	1:1	1:1	1:1	1:1
RR	60	23	23	60	30	30	60	60	60
MAP	89±7.3	80±13.4	51±23 <sup>*</sup>	98.2±13	44±11	49±11	113±9.2	113±9.2	94±20
pH	7.28±0.0	7.32±0.1	7.22±0.1 <sup>*†</sup>	7.31±0.0	7.31±0.0	7.32±0.0	7.30±0.0	7.30±0.0	7.28±0.0
PaO <sub>2</sub>	95±1.5	96.5±9	41.2±7.5 <sup>*†</sup>	92.4±14.7	114.3±6.5	126±9.6	84.6±7	87.5±8.5	84±7.9
PaCO <sub>2</sub>	41.4±5.4	37.5±9.3	36.3±10.2	44.2±3.2	39.6±5.3	36±1.8	46.4±1	48.2±7.4	50.5±4.6
Weight	340±26			320±30			310±14		

Ventilator parameters, arterial blood pressure and arterial blood gases at the start and end of each experiment. All experiments were terminated at 20 min. Experimental groups were (Peak Airway Pressure/Positive End-Expiratory Pressure): 45/0, 45/10 and 10/3. Baseline measurements were made before randomization. Statistical Comparisons: between-group comparisons are between 45/0 vs. 45/10 only (10/3, are control experiments for inspection; n=2). \*P<0.05 vs. 0 min; †P<0.05 vs. 45/10. **Abbreviations:** P<sub>AW</sub> Airway Pressure (cmH<sub>2</sub>O), V<sub>T</sub> Tidal Volume (mL/kg); P<sub>Insp</sub> Inspiratory Pressure (cmH<sub>2</sub>O); C<sub>Dyn</sub> Dynamic Compliance (mL/cmH<sub>2</sub>O); RR Respiratory Rate; I:E Inspiration: Expiration Ratio; MAP Mean Arterial Pressure (mmHg); pH Arterial pH; PaO<sub>2</sub> Arterial PO<sub>2</sub> (mmHg); PaCO<sub>2</sub> Arterial PCO<sub>2</sub> (mmHg); Weight (gm).

**Table 4 Supplement: Transpulmonary Pressures in Inspiration and Expiration (Series 4)**

	45/0 (n = 5)			45/10 (n = 5)			10/3 (n = 2)		
	Baseline	0 min	20 min	Baseline	0 min	20 min	Baseline	0 min	20 min
<b>P<sub>L</sub> Inspiration</b>	5.5±1.5	37.7±2.1 <sup>†</sup>	39.2±2.0 <sup>†</sup>	3.8±1.9	33.4±2.1	35.3±2.5	3.1±1.1	3.1±0.9	4.5±0.9
<b>P<sub>L</sub> Expiration</b>	0.2±1.4	-1.74±0.9 <sup>†</sup>	-2.2±0.9 <sup>†</sup>	-1.4±1.9	2.8±1.2	3.8±1.2 <sup>*</sup>	-1.1±0.0	-1.1±0.2	-0.7±0.4
<b>Delta P<sub>L</sub></b>	5.3±0.4	39.5±1.4 <sup>†</sup>	41.4±2.0 <sup>†</sup>	5.2±0.5	30.6±1.6	31.5±1.5	4.2±1.1	4.2±1.1	5.2±0.5

Transpulmonary pressure were measured during inspiration and expiration at the start and end of all experiments. Delta P<sub>L</sub> was calculated as P<sub>L</sub> inspiration – P<sub>L</sub> expiration. All experiments were terminated at 20 min. Experimental groups were (Peak Airway Pressure/Positive End-Expiratory Pressure): 45/0, 45/10 and 10/3. Baseline measurements were made before randomization. Statistical Comparisons: between-group comparisons are between 45/0 vs. 45/10 only (10/3, are control experiments for inspection; n=2). <sup>\*</sup>P<0.05 vs. 0 min; <sup>†</sup>P<0.05 vs. 45/10. **Abbreviations:** P<sub>L</sub> Transpulmonary pressure.

**Table 5 Supplement – Hemodynamics during Left Ventricular Pressure Measurement (*Series 5*)**

	45/0 (n = 4)			45/10 (n = 4)			10/3 (n = 2)		
	Baseline	0 min	20 min	Baseline	0 min	20 min	Baseline	0 min	20 min
LVSP	122±10.1	111±6.9	60±23.2 <sup>*</sup>	147±5.4	89±37	99±30.3	152±13.5	151±14.7	128±22.1
LVSP-TM	119.4±10.3	108±8.1	58±22.5 <sup>*</sup>	142±7.7	83±38.5	93±29.7	147.9±13.5	147±14.7	123±20.4
LVEDP	11.45±1.7	12.6±1.6	16±4.6	13±3.2	11.5±4.5	10.7±4.4	13.7±3	13.3±2.5	15.5±2.9
LVEDP-TM	9.3±2.3	10.6±1.8	14.3±3.9 <sup>†</sup>	9.1±4.2	5.9±2.3	6.1±1.7	9.5±2.9	9±2.4	9.8±4.4
MAP	91±7	86±14.7 <sup>†</sup>	36±12.4 <sup>*</sup>	92±19.2	46±6	46.5±8.2	109±3.3	108±2	94±19.7
Left CPP	73±9.4	70±19.5 <sup>†</sup>	16±13.1 <sup>*</sup>	70±12.3	29±9.2	30.5±5.8	83±3.1	82±4.8	74±14.3

Left ventricular pressure, systemic arterial pressure and left coronary perfusion pressure at the start and end of all experiments. Experimental groups were (Peak Airway Pressure/Positive End-Expiratory Pressure): 45/0, 45/10 and 10/3. All experiments were terminated at 20 min. Statistical Comparisons: between-group comparisons are between 45/0 vs. 45/10 only (10/3, are control experiments for inspection; n=2). <sup>\*</sup>P<0.05 vs. 0 min; <sup>†</sup>P<0.05 vs. 45/10. **Abbreviations:** LVSP Left Ventricular Systolic Pressure (mmHg); LVSP-TM Transmural Left Ventricular Systolic Pressure (mmHg); LVEDP Left Ventricular End-Diastolic Pressure (mmHg); LVEDP-TM Transmural Left Ventricular End-Diastolic Pressure (mmHg); MAP Mean Systemic Arterial Pressure (mmHg); Left CPP Left Coronary Perfusion Pressure (mmHg).

*KATIRA ET AL – ON-LINE SUPPLEMENT*

**Statistical Analysis:** Statistical analysis were performed using SigmaPlot 12 (Systat Software Inc., UK). Parametric tests ( $t$ -test and ANOVA) were used to compare groups and repeated measures ANOVA (followed by  $t$ -tests, where appropriate) was used to determine effects over time.